Multi-Objective Optimization of a Leg Mechanism Using Genetic Algorithms

Kalyanmoy Deb and Santosh Tiwari
Department of Mechanical Engineering
Indian Institute of Technology Kanpur
Kanpur, PIN 208016, India
Email: {deb,tiwaris}@iitk.ac.in
http://www.iitk.ac.in/kangal/deb.htm

KanGAL Report Number: 2004005

Abstract

Many engineering optimal design problems involve multiple conflicting objectives and often they are attempted to be solved by converting them into a single composite objective. Moreover, to be able to use standard classical optimization methods, often such problems are divided into suitable subproblems and solved in stages. A leg mechanism design problem which received some attention in the past involves link length and spring characteristics as decision variables and as many as three objectives and 17 inequality constraints. The problem is difficult to optimize due to strict geometric constraints which make only a tiny fraction of the search space feasible. In this paper, we apply an evolutionary multi-objective optimization (EMO) methodology to solve the complete leg mechanism optimization problem for all three objectives simultaneously. In the way of achieving to solve the complete problem, we demonstrate how such a complex engineering design problem can be solved by evolutionary algorithms and useful insights about the design problem can be obtained by systematically starting with fewer objectives and gradually adding more objectives. Several optimization concepts are introduced to gain confidence in obtained solutions. Results of this study are compared with that of an earlier study and in all cases the superiority and flexibility of the EMO approach is demonstrated. The ease and efficiency of EMO methodology demonstrated in this paper should encourage similar other studies involving other mechanical component design problems.

1 Introduction

It has been increasingly understood that most engineering optimal design problems involve simultaneous optimization of multiple conflicting objectives. Recently, a study (Shieh et al., 1996) considered optimizing a two degree-of-freedom (DOF) leg mechanism consisting of a four-bar linkage and a pantograph and three different objectives were used. The design objectives considered were the minimization of the total frontal area needed for the leg mechanism (called the leg-size), the peak crank torque required to operate the mechanism, and the vertical actuating force. It was further shown that by using a number of light-weight and passive spring elements, the required force and torque can be reduced. The problem has a number of geometric constraints which make it challenging to solve by any optimization method. The study used a two-stage optimization model for the purpose. In the first stage, the leg dimensions were optimized for all three design objectives by converting them into a single combined objective. However, the introduction of spring elements in the second stage increased the number of design variables and the study resorted to finding optimal spring details alone by keeping the leg dimensions to their optimal

values obtained in the first stage. In various other complex engineering design problems, such a division of the overall problem into two or more subproblems suitable for optimization is routinely performed mainly due to the lack of suitable optimization techniques.

In this paper, we present a genetic-algorithm (GA) based approach for the complete design of the same compound mechanism with spring elements. Moreover, the GA approach can handle multiple objectives simultaneously, without requiring the objectives to be combined to a single one (Deb et al., 2002). The approach uses a constraint-handling strategy which does not require any penalty parameter and is particularly designed to work with a population-based optimization approach (Deb, 2000). To understand the optimization problem better, we first treat the leg mechanism without the tension springs. Starting with two objectives of design, we systematically consider all three objectives. In addition to finding the resulting Pareto-optimal solutions, we also analyze them to unveil any salient properties associated with them. Such information, if exist, are useful to a designer and are difficult to find by other means (Deb, 2003).

We observe that the minimization of peak crank torque (suggested and used in the earlier study (Shieh et al., 1996) (henceforth we call it the original study)) is not a particularly useful one in this problem, because it only denotes the maximum torque requirement and does not represent the same for the entire cycle of operation. Here, we suggest minimizing the energy requirement instead of the peak crank torque and interesting Pareto-optimal solutions are found.

Finally, we consider the spring-loaded leg mechanism and treat all variables (link geometries and spring details) as design variables. Such considerations increase the number of constraints and make the problem more difficult to solve. By using the same EMO strategy and other concepts of multi-objective optimization, we show how a complex engineering optimization problem can be solved systematically and in a more meaningful manner.

The organization of this paper is as follows. In section 2, we review the problem description without tension springs attached to the leg mechanism. In section 3, we discuss the optimization methodology. In section 4 the optimization results are discussed for the first case where tension springs are not introduced. In section 5 we discuss the problem with tension springs attached to the leg mechanism. In section 6 the optimization results for the second case has been discussed and these results are compared with the first case. Finally, in section 7 we present a summary of all solutions reported in the study. Section 8 presents the Appendix which includes additional formulation of the design variables for the problem.

2 Formulation of the Leg Mechanism

A planar two degree-of-freedom leg mechanism (Williams et al., 1991) composed of a four-bar crank rocker $ABCD$ and a pantograph $EFGHIJ$ is shown in Figure 1. The link AB is the crank and is driven by a motor located at A. The motion of crank AB constitutes the first degree-of-freedom of the system. The link BCE is the connecting rod and point E on this link generates an *ovoid* path which is used by the pantograph $EFGHIJ$ for normal walking on a flat terrain. In the figure, links BC, CD, CE have identical lengths. The angle between DA and the symmetry axis DH is $\phi/2$ which is half of the angle between BC and CE (which is ϕ). For such a four-bar crank rocker, the path traced by the coupler point E is symmetric about the axis DH (Hartenberg and Denavit, 1964).

The pantograph $EFGHIJ$ is connected to the four-bar linkage at point E and thus the motion of point E serves as the input for the pantograph which in turn generates a similar path at the point J which is called the foot point. The pantograph generates an exactly similar curve but magnified by a factor of $(-x_5/x_4)$. The negative sign implies that the curve is inverted at point J. The curve traced by point J has two extremes in the X direction, J_1 and J_3. The path comprising of the curve $J_1J_2J_3$ is the propelling motion of the foot path and the rest is the returning portion of the path. Due to symmetry of the coupler point path E and the geometry of the pantograph

points J_1 and J_3 are also symmetric about the symmetry axis BH (Hartenberg and Denavit, 1964).

To find the optimal operating conditions, we consider three objective functions: (i) the peak crank torque required to operate the mechanism for one complete cycle, (ii) vertical actuating force required at point H, and (iii) the normalized leg-size, defined as the overall frontal area needed for the leg mechanism compared to the rectangular space within which the foot point is allowed to move. For determining the normalized leg-size, we consider a prerequisite vertical stride and horizontal stride. The leg-size is normalized based on the stride of the mechanism. Apart from the objective functions we also consider various constraints on the geometry of the mechanism to ensure a smooth operation with a minimal fluctuation in the operating parameters. We also consider certain space constraints in order to ensure a proper foot path. For a detailed description of the problem refer to the earlier study (Shieh et al., 1994). Here we provide a brief overview of the design problem. Five length variables (x_1 to x_5) and one angle variable ($x_6 = \phi$), as shown in Figure 1, are used in the first stage optimization.

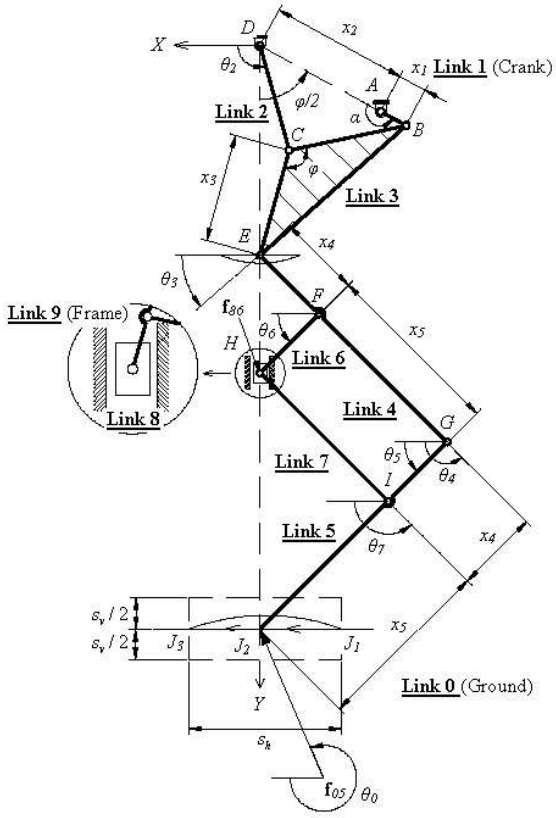

Figure 1: A Schematic of the leg mechanism without any spring element.

2.1 Optimization Problem Formulation

In this section, we present the objective functions and constraints involved in the first part of the problem.

2.1.1 Objective Functions

Objective 1: Minimizing the vertical actuating force. The vertical actuating force is the force that acts at the joint H. This comes into action because of the vertical component of the ground reaction force. We neglect the inertia effect of the links and also assume that the motion is slow,

so that acceleration of any link can be neglected. Hence one design objective is to minimize the vertical actuating force:

$$F(\mathbf{x}) = \left(1 + \frac{x_5}{x_4}\right) f_{50Y}, \tag{1}$$

where f_{50Y} is the force applied by link 5 to the ground and is equal to $-f_{05Y}$, shown in the figure.

Objective 2: Minimizing the normalized leg-size. We define the leg-size as the maximum length multiplied by maximum width of the entire leg mechanism. As the mechanism operates, the point E moves along the path shown in Figure 1 and the height and width of the leg mechanism changes. We compute the leg-size when the point E (and hence J) is on the axis of symmetry. This choice of leg-size simplifies the calculation significantly. This particular configuration is shown in the figure. Also, we choose $EG = GJ$ for the pantograph and choose the pantograph transmission angle ($\angle\ BCD$) as $\pi/2$ for this configuration. At this configuration, we also note that the variable $\alpha = \pi$. We define the length of the leg as maximum distance between the points D and J. At the configuration given in the figure we have the following:

$$\begin{aligned} l &= DE + EJ, \\ &= Y_E\mid_{\alpha=\pi} + \sqrt{2}(x_4 + x_5). \end{aligned} \tag{2}$$

A general variation of Y_E with α can be found at the Appendix. The width of the leg mechanism may be defined as the maximum numerical value of the x-coordinate of point B or G depending upon which is larger. Hence the width is given by:

$$w = \max\left((x_1 + x_2)\sin\left(\frac{\phi}{2}\right), \frac{(x_4 + x_5)}{\sqrt{2}}\right). \tag{3}$$

With the above computations of length and width of the leg mechanism, we now define the *normalized leg-size* as the ratio of frontal area of leg mechanism to the ratio of product of prescribed horizontal and vertical strides, marked as s_h and s_v, respectively. Thus, the next objective is to minimize:

$$\begin{aligned} S(\mathbf{x}) &= \frac{lw}{s_v s_h}, \\ &= \frac{\left(Y_E\mid_{\alpha=\pi} + \sqrt{2}(x_4 + x_5)\right)\max\left((x_1 + x_2)\sin\frac{\phi}{2}), \frac{x_4+x_5}{\sqrt{2}}\right)}{s_v s_h}. \end{aligned} \tag{4}$$

Objective 3: Minimizing the peak crank torque. In order to compute the required torque we proceed as follows. We assume that the links are mass-less, thereby neglecting the inertia effect of the mechanism. We also assume that there is no power transmission loss, hence the power input equals the power output. Since the power input is $T\frac{d\alpha}{dt}$ and the power output is $\left(f_{50X}\frac{dX_J}{dt} + f_{50Y}\frac{dY_J}{dt}\right)$, we have the following:

$$T(\mathbf{x}, \alpha) = f_{50X}\frac{dX_J}{d\alpha} + f_{50Y}\frac{dY_J}{d\alpha}, \quad \forall \alpha \in R_P. \tag{5}$$

The above equation of torque is valid for the propelling portion (R_P) of the cycle. This is because during the returning motion, the foot point will loose contact with the ground and hence no torque would be required to be supplied. It is to be noted that the motion of the slider will not affect the torque requirement. To find the expression for X_J and Y_J, we assume that the slider is held at its mid-range position.

The formulation for $T(\mathbf{x}, \alpha)$ can be found at the Appendix. To compute the third objective denoting the peak crank torque, we simply find the maximum value of $T(\mathbf{x}, \alpha)$ for the entire propelling portion of α:

$$T(\mathbf{x}) = \max_{\alpha \in R_P} T(\mathbf{x}, \alpha). \tag{6}$$

2.1.2 Constraint Functions

Here, we present all constraints required to have a smooth operation of the leg mechanism.

Constraint on stride length: The horizontal stride is defined as the distance in the x-direction between the two extreme points J_1 and J_3. These points are equidistant from the symmetry axis and can be obtained by equating $dX_J/d\alpha = 0$. Hence the first constraint is:

$$g_1(\mathbf{x}) \equiv 2X_{J_1} - s_h \geq 0. \tag{7}$$

Constraint on foot-path height: The height of the foot path is defined as the difference between the minimum and maximum y-coordinate of the foot point J. This occurs at $\alpha = 0$ and $\alpha = \pi$, respectively. Hence the second constraint function is:

$$g_2(\mathbf{x}) \equiv \frac{Y_J|_{\alpha=\pi} - Y_J|_{\alpha=0}}{s_h} - H_{C2} \geq 0, \tag{8}$$

where H_{C2} is a permissible value of the first term of the above constraint. A value of $H_{C2} = 0.08$ was used in the original study and we also use the same value here.

Constraint on four-bar transmission angle: An ideal value of the transmission angle ($\angle BCD$) is 90 degrees. Hence we put two constraints on the actual transmission angle such that it does not fluctuate much from 90^o.

$$g_3(\mathbf{x}) \equiv 2\sin^{-1}\left(\frac{x_2 - x_1}{2x_3}\right) - H_{C3} \geq 0, \tag{9}$$

$$g_4(\mathbf{x}) \equiv -2\sin^{-1}\left(\frac{x_2 + x_1}{2x_3}\right) + H_{C4} \geq 0. \tag{10}$$

The parameters H_{C3} and H_{C4} are chosen such that $(\pi/2 - H_{C3}) = (H_{C4} - \pi/2)$ and $H_{C3} = 0.873$ (Shieh et al., 1996). We use the same values here. Moreover, these two constraints ensure that the Grashof criterion (Ghosh and Mallik, 1988) is satisfied.

Constraint on pantograph transmission angle: The transmission angle in this case is defined as the $\angle EGJ$. Again, an ideal value for this angle is 90^o and two constraints are added to make sure that the transmission angle does not deviate much from 90^o.

$$g_5(\mathbf{x}) \equiv \cos^{-1}\left(\frac{2(x_4 + x_5)^2 - l_{min}^2}{2(x_4 + x_5)^2}\right) - H_{C5} \geq 0, \tag{11}$$

$$g_6(\mathbf{x}) \equiv -\cos^{-1}\left(\frac{2(x_4 + x_5)^2 - l_{max}^2}{2(x_4 + x_5)^2}\right) + H_{C6} \geq 0, \tag{12}$$

where l_{min} and l_{max} are the minimum and maximum values of EJ. We also have

$$l^2 = (X_J - X_E)^2 + (Y_J - Y_E)^2.$$

Knowing the coordinates of points E and J, the minimum and maximum values of l can be found numerically. As before, H_{C5} and H_{C6} are chosen such that $(\pi/2 - H_{C5}) = (H_{C6} - \pi/2)$ and $H_{C5} = 0.873$ (Shieh et al., 1996). Identical values are used here.

Constraint on orientation of links 4 and 5: To prevent the link 4 from interfering with the four-bar mechanism and the link 5 from being tangential to the ground, the angle θ_5 is restricted as follows:

$$g_7(\mathbf{x}) \equiv \theta_5 - H_{FC1} \geq 0, \quad \forall \alpha \in R_P. \tag{13}$$

A formulation of θ_5 can be found in the Appendix. A value $H_{FC1} = 0.436$ rad (Shieh et al., 1996) is used here.

Constraint on the foot path curvature: For the leg mechanism to operate properly, it is required that the propelling portion of the path lies below the returning portion of the path. That is, we

need the propelling portion of the foot path concave upward (in the negative y-direction). Thus, we have the following constraint:

$$g_8(\mathbf{x}) \equiv -\frac{d^2 Y_J}{d\alpha^2} \geq 0, \quad \text{over } J_1 J_2 J_3. \tag{14}$$

With the above description of the objective functions and constraints, we now present the following multi-objective optimization problem for the leg mechanism without any spring element:

$$\begin{array}{rl} \text{Minimize} & \text{Force } F(\mathbf{x}) \quad \text{(Eqn. 1)}, \\ \text{Minimize} & \text{Leg-size } S(\mathbf{x}) \quad \text{(Eqn. 4)}, \\ \text{Minimize} & \text{Torque } T(\mathbf{x}) \quad \text{(Eqn. 6)}, \\ \text{subject to} & \text{Constraints } g_1(\mathbf{x}) \text{ to } g_8(\mathbf{x}) \text{ given in Eqns. 7 to 14}, \\ & 0.0 \leq x_i \leq 0.3 \text{ m} \quad \text{for } i = 1, 2, \ldots, 5, \\ & 0.0 \leq \phi \leq 3.0 \text{ rad}. \end{array} \tag{15}$$

The above optimization problem involves six decision variables, three non-linear objective functions, and eight non-linear inequality constraints. Each variable is also bounded within a lower and an upper limit. The non-linearity and multiplicity in the objective function and constraints provide the main difficulty in solving the problem. A set of randomly generated solutions over the above-mentioned variable bounds indicate that about only one in 10^4 solutions is feasible. Such a severity of the feasible region makes the problem even more difficult to solve. In the following, we briefly mention the optimization method used in this study and thereafter present simulation results.

3 Optimization Methodology

To handle multiple objective functions, we use an evolutionary multi-objective optimization method, commonly known as the *elitist non-dominated sorting genetic algorithm* (or NSGA-II) (Deb et al., 2002). We use a C-code developed by the first author and his students at the Kanpur Genetic Algorithms Laboratory (KanGAL) and the code is available from the web site `http://www.iitk.ac.in/kangal/soft.htm`. NSGA-II uses a ranking of *dominated* solutions in a population to ensure progress towards the Pareto-optimal front and a *crowding* operator to ensure a good diversity among obtained solutions. For details, readers may refer to the original NSGA-II study (Deb et al., 2002). The NSGA-II has a number of advantages:

1. NSGA-II can find a number of Pareto-optimal or near-Pareto-optimal solutions simultaneously in one simulation run.
2. NSGA-II does not demand any new parameters to be supplied by the user.
3. NSGA-II uses an efficient constraint-handling technique based on constraint-domination operator (Deb, 2001).
4. NSGA-II can be used to solve any number of objectives with an iteration-wise complexity of $O(MN^2)$, where M is the number of objectives and N is the number of solutions used in a NSGA-II population.

In this study, we have used the following parameter values:

Population size:	$1000 \sim 2000$
Number of generations:	$1000 \sim 2000$
Crossover probability:	$0.4 \sim 0.95$
Real-parameter mutation probability:	$0.05 \sim 0.25$
Distribution index for crossover (Deb and Agrawal, 1995):	$10 \sim 40$
Distribution index for mutation (Deb and Goyal, 1998):	$50 \sim 150$

The reason of choosing the above range of values is as follows. The problem formulation described in the previous section indicates that the problem is highly non-linear and constrained, involving trigonometric terms. To focus on an appropriate set of parameters, we have experimented with a number of different settings and observed that the above setting worked the best. To have a good confidence on optimality of the obtained solutions, we have run NSGA-II from 10 different initial populations independently with randomly chosen parameter values in the above ranges. Thereafter, all non-dominated sets from 10 runs are combined together and the best non-dominated solutions are reported in each case. For solving difficult multi-objective optimization problems using evolutionary algorithms, it is suggested to use a hybrid approach in which the solutions obtained from an evolutionary algorithm are further processed by using a local search method (Deb, 2001). To achieve this, we first use a k-mean clustering algorithm (based on Euclidean distance of solutions in the objective space) and find a handful of wide-spread trade-off solutions out of the NSGA-II solutions. Thereafter, a genetic local-search (to optimize a combined weighted objective) is applied to each solution to check if any further improvement is possible. The solutions obtained after the local-search from each of the clustered solutions are declared as the obtained NSGA-II solutions.

The above hybrid NSGA-II procedure is a numerical optimization procedure. To gain confidence on the optimality of the obtained solutions, individual objectives are minimized using a real-parameter genetic algorithm (GA) (Deb, 2001) with identical genetic operators used in NSGA-II and are also plotted along with obtained NSGA-II solutions. In some problems, the ϵ-constraint optimization procedure (Deb, 2001; Miettinen, 1999), solved using a single-objective GA, is also used to gain further confidence.

We would like to highlight here that the above procedure of using an evolutionary multi-objective optimization (EMO) algorithm followed by several local search procedures and verifying the obtained solutions with multiple single-objective optimizations is a conceptually sound optimization procedure. Such a procedure utilizing several optimization concepts helps provide confidence on the reported results. We believe that such techniques are necessary particularly when a numerical optimization procedure (without a mathematical convergence proof) is used to solve a complex optimization problem.

4 Simulation Results

Simulation runs are performed for two as well as three objectives in a systematic manner. For the two objective cases, we consider (i) the actuating force versus the normalized leg-size and (ii) the actuating force versus the peak crank torque. For the three objective case, all three objectives are considered simultaneously. A comparison of the obtained results is made with the corresponding results reported in the original study (Shieh et al., 1996). Before we present the NSGA-II results, we first tabulate the seven trade-off solutions reported in the original study. For one of the solutions, we found a discrepancy in objective values computed by our formulation and that of the original study. Using these decision variables, we recompute objective values using our formulation and present the corresponding values in Table 1. For the above results, the following parameter values were used:

Ground reaction forces:	$f_{50X} = 0$ N, $f_{50Y} = 890$ N
Horizontal stride:	$s_h = 0.3$ m
Vertical stride:	$s_v = 0.2$ m

We are now ready to present single-objective GA and multi-objective NSGA-II results.

Table 1: Optimized solutions from the original study.

	Design variables						Objective functions		
S.no.	x_1(cm)	x_2(cm)	x_3(cm)	x_4(cm)	x_5(cm)	ϕ(rad)	F(kN)	S	T(Nm)
1	5.0	21.3	19.3	13.8	23.0	2.20	2.37	3.87	8.40
2	4.5	19.4	17.3	12.4	23.1	2.17	2.55	3.49	8.12
3	4.1	17.8	15.6	11.2	23.4	2.14	2.75	3.22	8.05
4	3.7	16.4	14.3	10.1	23.7	2.09	2.98	3.01	7.93
5	3.4	15.6	13.0	9.1	24.1	2.05	3.25	2.82	7.87
6	3.1	15.4	12.5	8.3	24.8	2.00	3.55	2.77	7.91
7	2.9	14.5	11.8	7.7	25.5	2.00	3.84	2.73	8.01

4.1 Single-Objective GA Results

First, we perform the single-objective optimization of each of the three objectives using a real-parameter GA and present the results in Table 2. The first row presents the minimum solution

Table 2: Single-objective optimization results using a GA.

Obj. Fun.	Optimal Design Variables						Objective functions		
(minimized)	x_1(cm)	x_2(cm)	x_3(cm)	x_4(cm)	x_5(cm)	ϕ(rad)	F (kN)	S	T (Nm)
Force	8.60	30.0	25.30	28.56	30.0	2.29	*1.82*	8.88	17.22
Leg-size	1.00	4.94	4.60	2.79	22.8	2.25	8.17	*1.36*	9.17
Torque	6.77	30.0	25.86	23.14	30.0	2.11	2.04	7.83	*7.87*

corresponding to the minimization of actuating force. The obtained solution requires 1.82 kN force. For this solution, the corresponding leg-size and torque values are also tabulated. Similarly, the second and third rows present the minimization results of leg-size and torque, respectively. The trade-off among all three objectives is clear from the table. Each of the three objective functions has the minimum value for the case when the function was minimized.

4.2 Actuating Force and Leg-Size Minimization

Next, we consider two-objective minimizations. We apply NSGA-II to optimize the case with force and normalized leg-size as the design objectives and the resulting 10 trade-off solutions are presented in Table 3. For each of the ten solutions, the corresponding peak crank torque is also computed and presented in the table. To investigate the trade-off better, we plot the force and leg-size values in Figure 2 for all 10 solutions. To get a feel of the progress of NSGA-II from the initial generation, we have also plotted the feasible initial population members which lie in the domain of the plot in the figure. Interestingly, only five (out of 1,000) solutions are found to lie in the domain of the plot.

The NSGA-II solutions are also compared with those reported in the earlier study. It is clear from the figure that NSGA-II solutions outperform the earlier reported solutions. The trade-off front reported earlier is completely dominated by the trade-off front formed using NSGA-II solutions. Moreover, the extent of NSGA-II solutions along both axes is more than that for the earlier solutions.

Finally, the single-objective optimized solutions for force and leg-size minimizations (reported in Table 2) are also shown in the figure. NSGA-II is able to find a solution very close to the

Table 3: Minimization of force and leg-size using NSGA-II.

	Design Variables						Objective functions		
S.no.	x_1(cm)	x_2(cm)	x_3(cm)	x_4(cm)	x_5(cm)	ϕ(rad)	F (kN)	S	T (Nm)
1	8.50	29.98	25.40	27.01	28.52	2.27	1.83	8.17	16.10
2	7.46	28.68	25.08	21.12	24.44	2.20	1.92	6.01	10.56
3	6.85	27.09	23.92	18.92	23.60	2.19	2.00	5.31	9.58
4	5.89	24.16	21.60	15.91	22.79	2.19	2.17	4.38	8.83
5	5.15	22.05	19.92	13.66	22.15	2.19	2.33	3.76	8.28
6	4.34	18.50	16.61	11.60	22.45	2.19	2.61	3.21	8.46
7	3.71	15.76	14.23	9.89	22.25	2.19	2.89	2.76	8.37
8	3.04	13.48	12.15	8.13	22.34	2.19	3.33	2.39	8.37
9	2.39	13.68	13.26	6.96	22.70	2.31	3.79	2.37	9.63
10	2.03	13.85	13.48	6.09	23.29	2.32	4.30	2.35	9.99

minimum solution for the actuating force. However, NSGA-II is not able to find a solution close to the minimum solution for the normalized leg-size. Our conclusion from this study is that the minimization of the leg-size is a more difficult task in this problem than the minimization of the actuating force. The plot of these extreme optimal solutions clearly shows the limitation of the earlier study in finding the trade-off solutions.

4.3 Actuating Force and Peak Crank Torque Minimization

Next, we consider force and peak crank torque minimizations. The NSGA-II solutions are tabulated in Table 4. The corresponding leg-size values are computed and tabulated as well. A plot

Table 4: Minimization of force and peak crank torque using NSGA-II.

	Design Variables						Objective functions		
S.no.	x_1(cm)	x_2(cm)	x_3(cm)	x_4(cm)	x_5(cm)	ϕ(rad)	F (kN)	S	T (Nm)
1	6.85	29.70	26.11	20.86	26.08	2.14	2.00	6.45	7.98
2	6.16	28.10	23.62	18.85	27.41	2.06	2.18	6.05	7.73
3	5.05	23.88	19.84	13.84	25.72	2.03	2.54	4.40	7.68
4	5.50	26.30	21.85	14.50	26.35	2.03	2.75	4.91	7.67
5	4.84	23.57	19.66	12.46	26.28	2.02	3.00	4.24	7.67

of these solutions in the objective space is shown in Figure 3. Once again, the trade-off front obtained by NSGA-II solutions dominates that of the original study. Here, the hybrid NSGA-II procedure is able to find better solutions in terms of peak crank torque minimization than the single-objective GA minimization of the peak crank torque. We believe that peak crank torque is not a good measure of the overall torque required to operate the leg mechanism, since it represents the maximum required torque and does not necessarily represent the nature of torque variation over the entire cycle of operation of the leg mechanism. We discuss more about this issue in the next section. Nevertheless, this study shows the superiority of NSGA-II over the approach used in the original study.

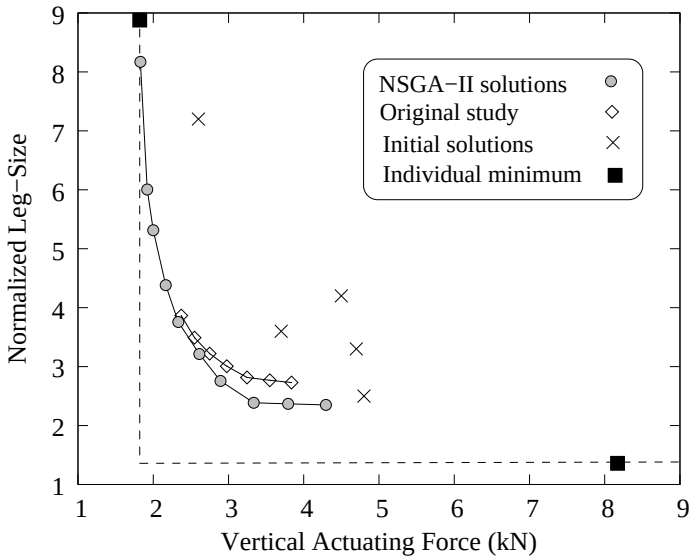

Figure 2: NSGA-II solutions compared with the original study and with single-objective GAs for force and leg-size minimizations.

4.4 Force, Leg-Size, and Peak Crank Torque Minimization

Next, we consider all three objectives in NSGA-II. The obtained solutions are shown in Table 5. Figure 4 compares these solutions with those obtained in the original study. It is important to

Table 5: Minimization of all three objectives using NSGA-II.

	Design Variables						Objective functions		
S.no.	x_1(cm)	x_2(cm)	x_3(cm)	x_4(cm)	x_5(cm)	ϕ(rad)	F (kN)	S	T (Nm)
1	6.02	25.83	23.24	16.59	23.10	2.19	2.13	4.75	8.20
2	5.14	22.19	19.71	13.75	23.01	2.16	2.38	3.89	8.16
3	4.66	20.03	17.83	12.35	22.41	2.17	2.50	3.42	8.12
4	4.46	19.66	16.94	11.79	23.11	2.11	2.63	3.37	7.93
5	3.71	16.33	14.08	9.74	22.95	2.11	2.99	2.83	7.92
6	3.49	15.64	13.39	9.21	23.65	2.09	3.18	2.80	7.81
7	3.10	14.07	11.91	8.12	23.34	2.07	3.45	2.50	7.79
8	2.95	13.19	11.22	7.77	23.32	2.09	3.56	2.40	7.88

highlight here that NSGA-II is capable of handling all three objectives simultaneously and the obtained solutions are not the outcome of multiple transformed single-objective optimizations, a procedure usually followed in multi-objective optimization studies. Here, we plot a set of representative solutions from the obtained Pareto-optimal front and compare with the solutions reported from the original study. For clarity, the projection of the trade-off front is also shown on the force-legsize plane in Figure 4. NSGA-II is able to find a better trade-off front than that of the existing study.

To investigate the plausible optimality of the obtained three-objective solutions, we plot the loci of the foot point coordinate for all eight solutions in Figure 5. It can be seen from the figure that all obtained solutions follow more or less a similar trajectory. Solutions with a smaller force requirement have a more flat propelling part of the walking cycle than those with a higher force

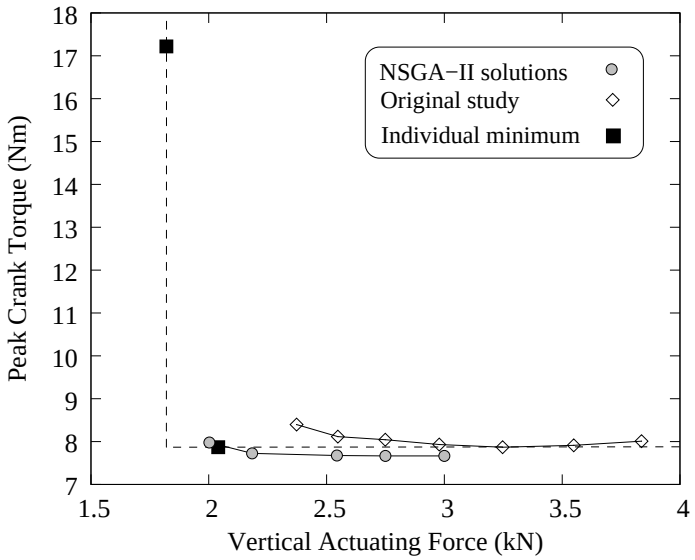

Figure 3: NSGA-II solutions are compared with the original study and with single-objective GAs for force and torque minimizations.

requirement. All solutions satisfy the prescribed horizontal and vertical stride limits, as shown in the figure.

To investigate the variation of torque $T(\mathbf{x}, \alpha)$ with crank angle α for all eight obtained solutions, we plot them in Figure 6. It is interesting to note that all eight solutions follow a certain pattern of torque requirement over the cycle. For solutions requiring smaller vertical actuating force, a larger torque is required in both positive and negative directions and vice versa. Interestingly, we observe the emergence of a pattern in the torque variation for different trade-off solutions.

Although Figure 6 shows the torque variation over the entire cycle of operation, what is being optimized is the peak crank torque – the maximum value of the torque variation in the entire propelling portion of the operation. As the figure shows, this happens at the smallest value of α for the propelling portion of the walking cycle. For clarity, the torque variation near the smallest α is enlarged and shown in the inset figure. Since the peak crank torque is not an ideal representative of the torque variation for the entire operating region, we use a different objective in the next section. Instead of using the peak crank torque, we compute the total supplied energy as

$$E(\mathbf{x}) = \int_{\alpha \in R_P+} T(\mathbf{x}, \alpha) d\alpha, \tag{16}$$

where R_P+ is the propelling portion requiring a positive torque value. A numerical integration (we have used the Romberg integration method with $\epsilon = 0.001$ here) must be used to compute the above objective value for a solution $\mathbf{x}$.

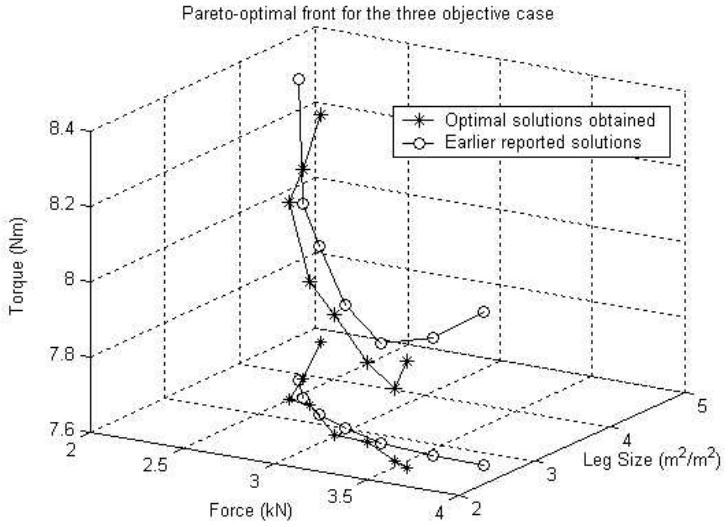

Figure 4: NSGA-II solutions compared with earlier study and single-objective GAs for force, leg-size and torque minimizations.

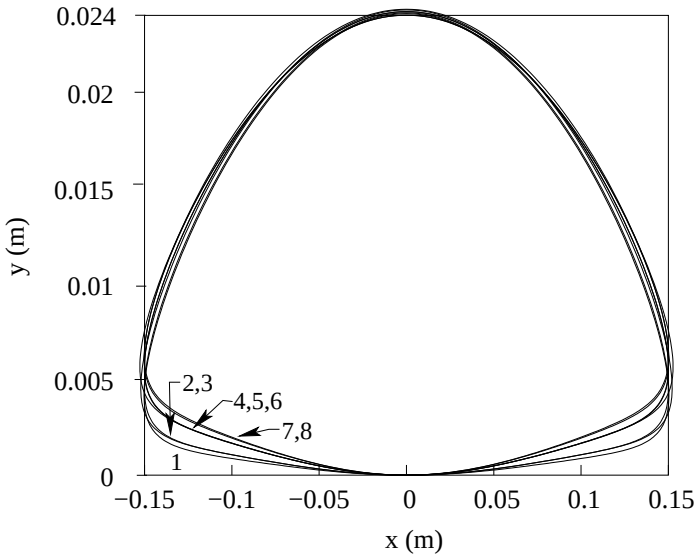

Figure 5: Variation of foot coordinate over an entire cycle for all eight obtained solutions.

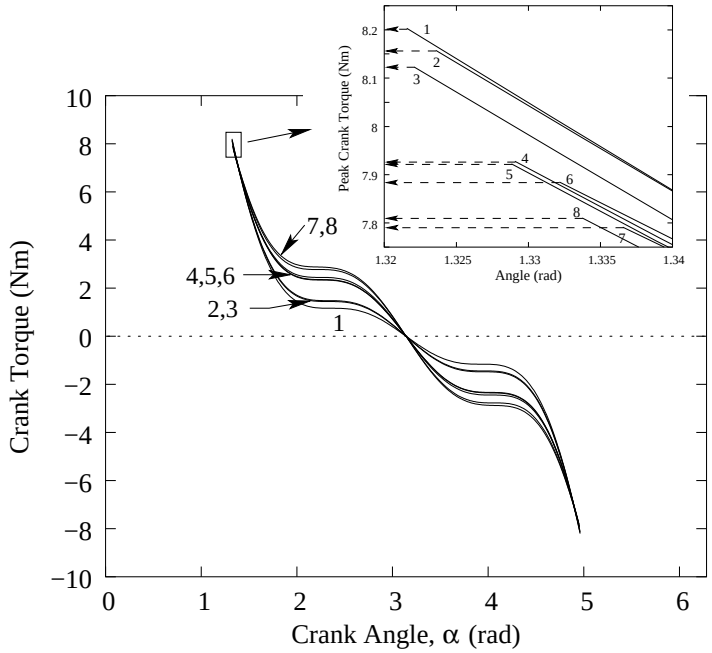

Figure 6: Variation of crank torque over the entire cycle for all eight obtained solutions.

4.5 Actuating Force and Energy Minimization

Next, we use NSGA-II to minimize the actuating force and the supplied energy computed as above. All eight constraints and variable bounds as mentioned before are used here as well. We have also used identical NSGA-II parameter values as used in the previous simulation. A number of well-spread Pareto-optimal solutions are shown in Table 6. Like before, we observe a conflicting

Table 6: Minimization of actuating force and supplied energy using NSGA-II.

	Design Variables						Objective functions		
S.no.	x_1(cm)	x_2(cm)	x_3(cm)	x_4(cm)	x_5(cm)	ϕ(rad)	F (kN)	S	E (J)
1	8.60	30.00	25.31	28.40	29.79	2.28	1.82	8.79	18.34
2	8.14	30.00	25.85	27.52	29.67	2.22	1.85	8.70	10.95
3	6.99	29.99	27.18	23.61	28.07	2.20	1.95	7.64	3.54
4	5.93	28.64	26.44	19.14	29.95	2.20	2.28	6.98	2.91
5	5.53	28.19	25.77	16.44	30.00	2.17	2.51	6.34	2.88

nature of the two objectives. A plot of the entire Pareto-front obtained along with locus of foot-path for a few selected solutions (presented in Table 6) is given in Figure 7. We make a number of observations from this figure:

1. The obtained front seems to have a *knee* solution (marked as 'knee' in the figure). This solution is marked as solution 3 in Table 6. Knee points are of utmost importance to a decision-maker, because for this solution a small gain in any one objective requires a large sacrifice in other objectives. Figure 7 depicts the same in either direction of the knee point. A knee point are of particular interest for implementation, because there is not much motivation to move away from this point. In this problem, NSGA-II has discovered one such point.

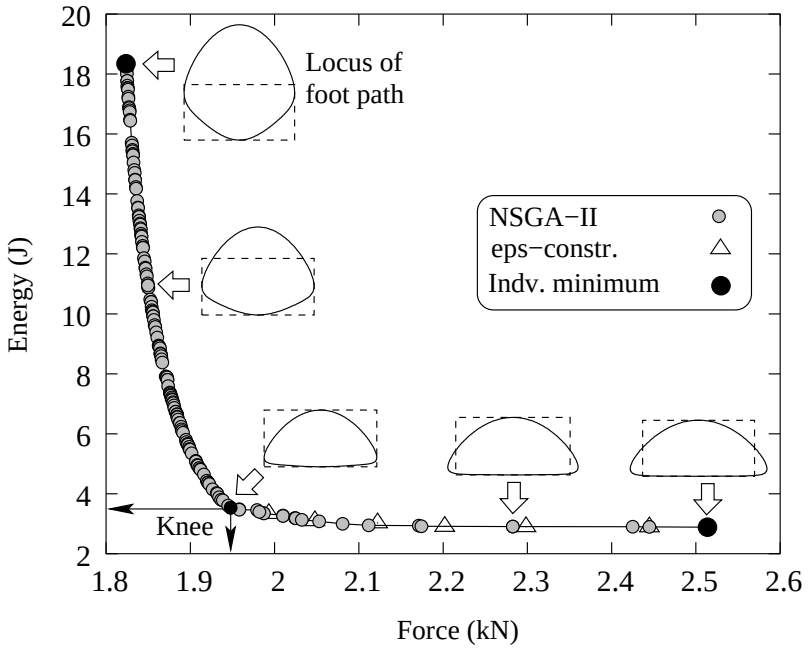

Figure 7: Energy versus actuating force minimization using NSGA-II (shaded circles). Single-objective minimum solutions are shown in solid circles and are found to be two extreme solutions of the obtained front. Moreover, a few optima (shown in triangles) of an ϵ-constraint formulation of the problem are also found to lie on the obtained front. Dashed boxes mark the limiting horizontal and vertical strides.

2. The solutions to the left of the knee point (that is, solutions requiring a smaller actuating force) possess a particular property: The foot is bounded by the allowable horizontal limit, while exceeding the allowable vertical limit. This makes the constraint g_1 active. Figure 8 plots the values of constraints g_1 and g_2 for all obtained solutions. It is clear that for solutions to the left of the knee point, constraint g_1 is active (that is, $g_1(\mathbf{x}) = 0$).

3. On the other hand, the solutions to the right of the knee point (that is, solutions requiring smaller energy) possess a different property. The foot movement is bounded by the allowable vertical limit and horizontal span exceeds the allowable limit, as shown in Figure 7. The constraint g_2 is active for these solutions. Interestingly, for the knee solution, both allowable horizontal and vertical limits are exactly satisfied (see Figure 8).

To gain more confidence about the optimality of the obtained Pareto-optimal front, next we solve several ϵ-constraint optimization problems:

$$\begin{array}{rl} \text{Minimize} & \text{Energy, } E(\mathbf{x}), \\ \text{subject to} & \text{Actuating force, } F(\mathbf{x}) \leq f_\epsilon, \\ & \text{Constraints } g_1(\mathbf{x}) \text{ to } g_8(\mathbf{x}) \text{ given in Eqns. 7 to 14,} \\ & 0.0 \leq x_i \leq 0.3 \text{ m} \quad \text{for } i = 1, 2, \ldots, 5, \\ & 0.0 \leq \phi \leq 3.0 \text{ rad.} \end{array} \tag{17}$$

We use five different f_ϵ values and solve the above single-objective optimization problem using a real-parameter GA. A standard tournament selection operator and an identical recombination operator (SBX) and mutation operator similar to the one used with NSGA-II are also used here. The corresponding optimum solutions are shown in Figure 7 with triangles. In addition, we have individually minimized each of the objective functions (with constraints and variable bounds

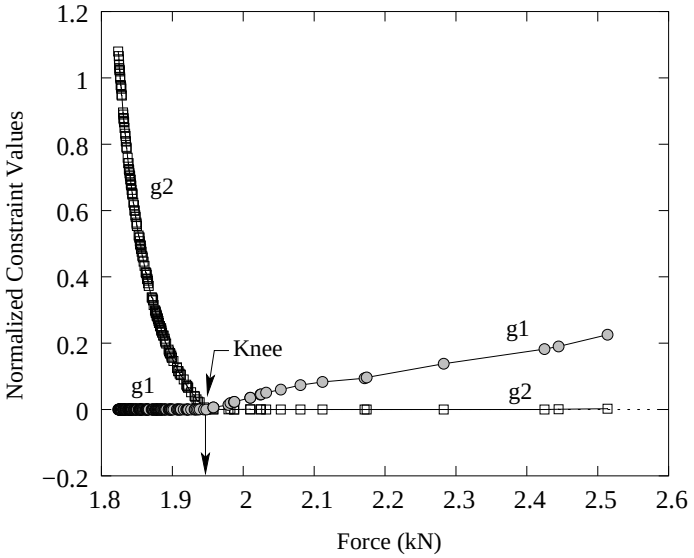

Figure 8: Constraint values of g_1 and g_2 are shown for all obtained NSGA-II solutions.

as given in Eqn. 17) using the same single-objective GA and obtained two different solutions, which are marked with a solid circle in the same figure. The fact that all these single-objective solutions fall more or less on the obtained two-objective NSGA-II solutions (shown in shaded circles) provides confidence about the efficacy of the NSGA-II algorithm in solving such complex multi-objective optimization problems.

4.5.1 Properties of Pareto-Optimal Solutions

In the above section, we have demonstrated how NSGA-II can be used to consider more than one objectives in a complex engineering design and a set of near Pareto-optimal solutions can be obtained. Getting the trade-off among conflicting objectives is an important matter. In this section, we discuss an even more important aspect associated with the obtained trade-off solutions.

It has been discussed elsewhere (Deb, 2003) that since all true Pareto-optimal solutions must satisfy a set of optimality conditions for a multi-objective optimization (Deb, 2001; Ehrgott, 2000; Miettinen, 1999), one may expect some *common properties* associated with the Pareto-optimal solutions. To investigate whether there exist any such property with the solutions of the entire Pareto-optimal solutions here, we plot four decision variables in Figure 9. Monotonic reductions in variables x_1 and x_2 (except two solutions) with an increased force requirement are interesting. The variable x_1 varies within 10% of the allocated search region ($x_1 \in [0, 30]$ cm) for the entire set of obtained solutions, whereas the variable x_2 varies within 6% of the allocated range. However, the large force requirement is compensated by an increased requirement of the link length 3 (or x_3). The variable x_3 also varies within 6.2% of the allocated search region. Interestingly, near the knee solution, the required angle ϕ has a minimum. However, over the entire range of Pareto-optimality, the angle ϕ varies between 125 to 130 degrees (varying within only 3% of the allocated search range). Thus, it can be concluded that the leg mechanism optimization problem is a difficult problem to solve, as even for two objectives the range of Pareto-optimal solutions is within a small region of the allocated search space. NSGA-II is able to find the trade-off optimal solutions in the narrow search region and discover interesting pattern of the change in variables with a monotonic increase in one of the objectives.

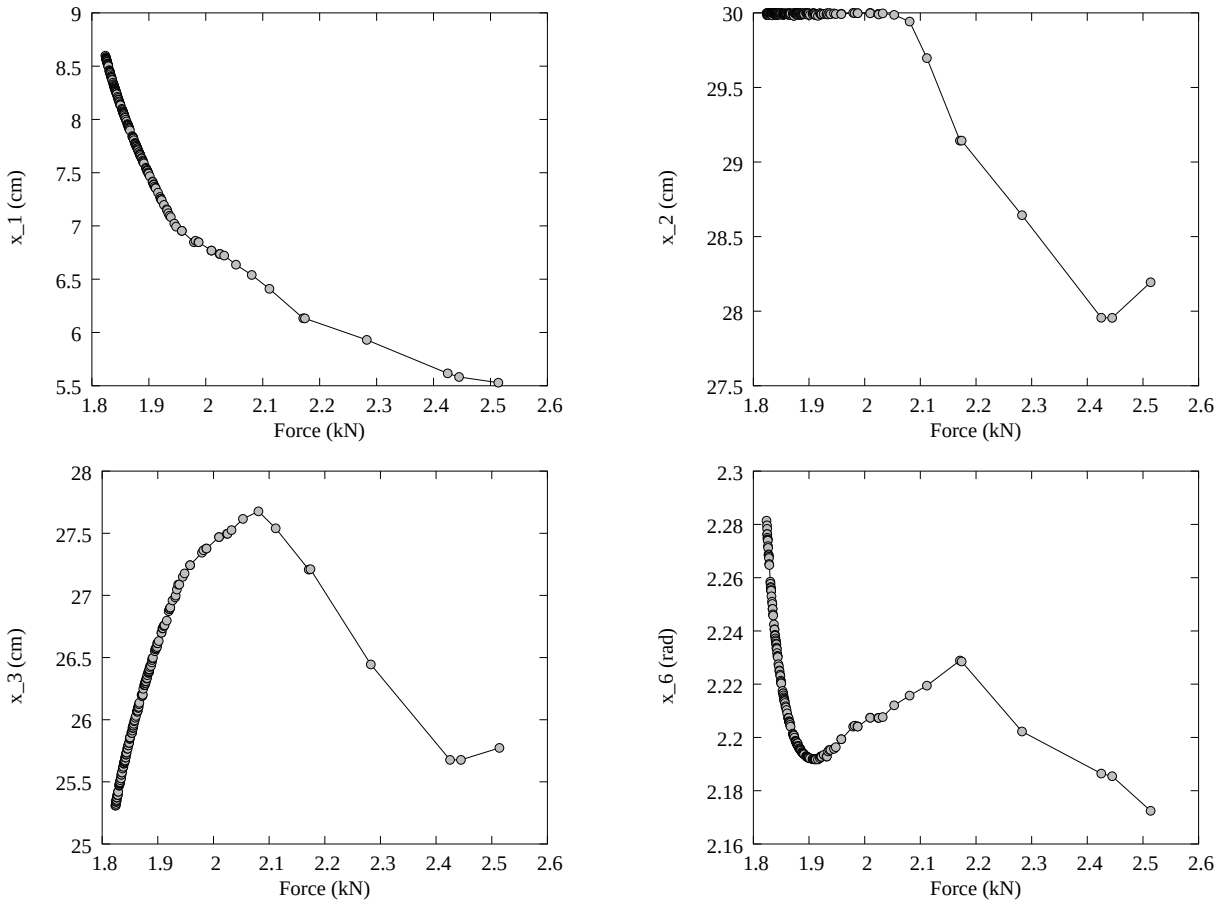

Figure 9: Variation of x_1, x_2, x_3 and x_6 are shown for all obtained solutions.

5 Leg Mechanism With Tension Springs

To reduce the force and torque requirements on the leg mechanism, an improved design can be achieved by using tension springs at a few locations on the original leg mechanism. When the springs are attached to the leg mechanism (as shown in Figure 10), the expressions for the vertical actuating force and torque change. The expression for leg-size however remains the same since the springs attached to the mechanism do not increase the length or breadth of the compound system. Springs are used to further reduce the vertical actuating force and peak crank torque required to operate the leg mechanism (Shieh et al., 1996). The original study considered three different spring configurations. For brevity, we use the configuration which was judged to be the best in that study.

In order to describe the optimization problem, we consider all link lengths along with the spring dimensions and their placement as design variables. Although this increases the number of variables, the optimized solution will certainly be as good or better than a two-stage optimization procedure adopted in the original study. That study did not consider the link lengths and angle ϕ as decision variables in the second stage and instead used one of the optimized solutions from the first stage study and considered the spring dimensions and their locations as decision variables. Since GAs (hence NSGA-II) are more flexible search procedures, we use all parameters (all six variables used earlier and spring dimensions and their locations) as variables.

In the following, we again formulate the new design problem having all previous constraints. The formulation for the leg-size remains the same as before. The new problem will however have certain new constraints due to the addition of tension springs and certain constraints which were

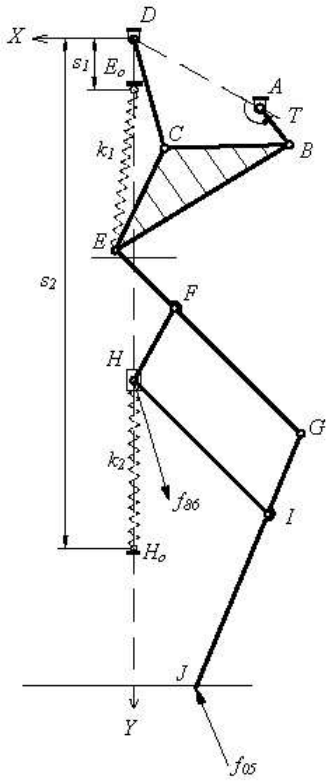

Figure 10: A schematic of the spring-loaded leg mechanism.

not considered in the original study (Shieh et al., 1996). These new constraints would ensure compatibility between the solution obtained and the physics of the problem.

The total number of variables now becomes 12. The number of objective functions is three and the number of constraints increases to 13.

5.1 Objective Functions

Here, we describe the modified objective functions for the spring-loaded leg mechanism.

Objective 1: Minimizing the vertical actuating force. The expression for the vertical actuating force in presence of springs is given by:

$$F(\mathbf{x}) = -\left(1 + \frac{x_5}{x_4}\right) f_{05Y} - k_2 \left((s_2 - Y_H) - l_{02}\right). \tag{18}$$

The derivation of $F(\mathbf{x})$ can be found in an earlier study (Shieh et al., 1994). Unlike in the previous stage, the actuating force is present even when the ground reaction force is zero. This is because a part of the force which is compensated by the spring during the propelling portion of the path is returned back during the returning portion of the path. The spring actually reduces the required vertical actuating force by a requisite amount. In the remaining portion of the path the same requisite amount of force starts acting in the opposite direction. Hence here again we have to consider the maximum actuating force from the above expression for the propelling portion or the returning portion of the path.

Objective 2: Minimizing the normalized leg-size. The expression for the leg-size remains the same since the addition of springs does not alter the leg-size.

Objective 3: Minimizing the peak crank torque. The expression for the peak crank torque is

given by:

$$T(\mathbf{x},\alpha) = \left(\frac{x_5}{x_4} f_{05X} + k_1 \delta_1 X_E\right) \frac{dX_E}{d\alpha} + \left(\frac{x_5}{x_4} f_{05Y} + k_1 \delta_1 \left(Y_E - s_1\right)\right) \frac{dY_E}{d\alpha}. \tag{19}$$

Here, $\delta_1 = \left(1 - \frac{l_{01}}{l_1}\right)$ and $l_1^2 = X_E^2 + (Y_E - s_1)^2$.

The derivation of $T(\mathbf{x},\alpha)$ can be found in an earlier study (Shieh et al., 1994). In the previous stage, as the leg is detached from the ground the torque is reduced to zero; hence the peak crank torque was found only for the propelling portion of the cycle. Here, since the springs are attached, they compensate for the torque during the propelling portion of the motion and the peak crank torque must be computed considering the returning portion of the path as well. Hence, the peak crank torque in this case refers to maximum numerical value of $T(\mathbf{x},\alpha)$ that occurs during the entire cycle:

$$T(\mathbf{x}) = \max_{0 \le \alpha \le 2\pi} T(\mathbf{x},\alpha). \tag{20}$$

It is to be noted that reaction forces in the expression for the torque are active only for the propelling portion of the motion and are zero for the rest of the motion.

5.2 Constraint Functions

All the above constraints that have been defined in the previous section are still valid and are applicable to the current problem. There are certain additional constraints which arise because of attachment of tension springs.

Constraint on the extension ratio of the springs: Since we are using tension springs, we have to impose a condition on the minimum length of the spring so that it is always greater than or equal to its natural length. Similarly we also need to impose a condition on the amount of extension that it can withstand.

For spring 1:

$$g_9(\mathbf{x}) \equiv \frac{\min\left(l_1\right)}{l_{01}} - H_{SC1} \ge 0, \tag{21}$$

$$g_{10}(\mathbf{x}) \equiv -\frac{\max\left(l_1\right)}{l_{01}} + H_{SC2} \ge 0. \tag{22}$$

For spring 2:

$$g_{11}(\mathbf{x}) \equiv \frac{\min\left(l_2\right)}{l_{02}} - H_{SC3} \ge 0, \tag{23}$$

$$g_{12}(\mathbf{x}) \equiv -\frac{\max\left(l_2\right)}{l_{02}} + H_{SC4} \ge 0. \tag{24}$$

In the above equations, we have used $l_1^2 = X_E^2 + (Y_E - s_1)^2$. Since X_E and Y_E vary during the motion, the minimum and maximum value for l_1 can be found numerically. Using above, we have the following equations:

$$\min\left(l_2\right) = s_2 - \left(Y_H + \frac{s_v}{2\left(1 + \frac{x_5}{x_4}\right)}\right),$$

$$\max\left(l_2\right) = s_2 - \left(Y_H - \frac{s_v}{2\left(1 + \frac{x_5}{x_4}\right)}\right).$$

In the above equations, we assume Y_H to be at its mid-range position.

Constraint on the location of spring attachment points: We also need to have constraints on the location of spring attachment points:

For spring 1:

$$g_{13}(\mathbf{x}) \equiv s_1 - H_{SC5} \geq 0, \tag{25}$$

$$g_{14}(\mathbf{x}) \equiv -s_1 + H_{SC6} \geq 0, \tag{26}$$

For spring 2:

$$g_{15}(\mathbf{x}) \equiv s_2 - H_{SC7} \geq 0, \tag{27}$$

$$g_{16}(\mathbf{x}) \equiv -s_2 + H_{SC8} \geq 0. \tag{28}$$

The spring 2 must not allow the attachment point H_o from interfering with the foot point J and also the obstacles that it may encounter during the motion. Since the foot-point J can lift itself to prevent it from obstacles, the constraint on point H_o restricting it to be located above the point J for the complete cycle will allow to achieve the above task. Hence we have the final constraint as follows:

$$g_{17}(\mathbf{x}) \equiv -s_2 + \min Y_J \geq 0. \tag{29}$$

This constraint was not considered in the original study, because the link dimensions were kept constant during the stage 2 optimization and thus the quantity $\min Y_J$ also remained constant.

With the above description of objective functions and constraints, we now present the following multi-objective optimization problem for the spring-loaded leg mechanism:

$$\begin{array}{ll}
\text{Minimize} & \text{Force } F(\mathbf{x}) \quad \text{(Eqn. 18)}, \\
\text{Minimize} & \text{Leg-size } S(\mathbf{x}) \quad \text{(Eqn. (4))}, \\
\text{Minimize} & \text{Torque } T(\mathbf{x}) \quad \text{(Eqn. 20)}, \\
\text{subject to} & \text{Constraints } g_1(\mathbf{x}) \text{ to } g_8(\mathbf{x}) \text{ given in Eqns. 7 to 14 and} \\
& \quad g_9(\mathbf{x}) \text{ to } g_{17}(\mathbf{x}) \text{ given in Eqns. 21 to 29}, \\
& 0.0 \leq x_i \leq 0.3 \text{ m} \quad \text{for } i = 1, 2, \ldots, 5, \\
& 0.0 \leq \phi \leq 3.0 \text{ rad} \\
& -0.3 \leq s_1 \leq 0.0 \text{ m}, \\
& 0.0 \leq s_2 \leq 0.7 \text{ m}, \\
& 0.0 \leq k_1, k_2 \leq 50 \text{ kN/m}, \\
& 0.0 \leq l_{01}, l_{02} \leq 0.5 \text{ m}.
\end{array} \tag{30}$$

Since s_1 and s_2 are decision variables in this problem, we treat constraints g_{13} to g_{16}, given in Eqns. 25 to 28, as variable bounds, thereby reducing the total number of constraints to 13.

6 Simulation Results for Spring-Loaded Leg Mechanism

Simulation runs are performed for two as well as three objectives. For the two-objective cases, we consider (i) actuating force versus normalized leg size and (ii) actuating force versus peak crank torque. For the three objectives case, all three objectives are considered simultaneously. A comparison is made with the results from stage 1. It is noteworthy that the original study did not perform the three-objective minimization and only executed the force-torque minimization.

The parameter values related to the leg mechanism are kept the same as before. The following parameters for the new constraints are chosen in agreement with the original study:

$$\begin{array}{llll}
H_{SC1} = 1.0, & H_{SC2} = 1.3, & H_{SC3} = 1.0, & H_{SC4} = 1.3, \\
H_{SC5} = -0.3, & H_{SC6} = 0.1, & H_{SC7} = 0.1, & H_{SC8} = 0.6.
\end{array}$$

The maximum natural length for any spring is 0.5 m and maximum spring constant for any spring is *50* kN/m.

6.1 Single-Objective Optimization Results

Simulation results for the single-objective optimization runs are given in Table 7. The trade-

Table 7: Single-objective minimization results using GAs for the spring-loaded leg mechanism.

S.no.	Force minimization	Leg Size minimization	Torque minimization
x_1 (cm)	4.02	3.89	3.81
x_2 (cm)	16.06	15.89	15.85
x_3 (cm)	14.18	14.18	14.2
x_4 (cm)	11.06	10.84	10.56
x_5 (cm)	23.55	23.52	23.35
ϕ (rad)	2.19	2.19	2.19
s_1 (cm)	-13.49	-13.42	-13.41
s_2 (cm)	68.87	69.07	68.87
k_1 (kN/m)	29.77	31.92	29.46
k_2 (kN/m)	40.85	42.11	41.75
l_{01} (cm)	38.24	38.29	38.07
l_{02} (cm)	22.80	23.28	23.29
F (kN)	*1.39*	1.41	1.43
S	3.10	*3.07*	3.00
T (Nm)	4.60	4.50	*4.27*

off among the optimal solutions is clear from the table. Except for the leg-size minimization, other two objective minimizations find smallest values in the respective objectives. As mentioned earlier, the minimization of the leg-size is a more difficult task for this problem.

6.2 Actuating Force and Leg-size Minimization

Next, we apply NSGA-II to solve the two-objective case of minimizing the force and normalized leg-size as design objectives and results are shown in Table 8. These solutions (stage 2 optimization results) are also plotted in Figure 11 and are compared with those obtained in the previous stage (without springs). The figure clearly demonstrates the benefits obtained by the introduction of springs in to the system. The addition of springs allows smaller actuating forces to be applied for a similar effect. A closer look at the solutions presented in Tables 3 and 8 will reveal that the link dimensions in stage 2 are much smaller than those obtained in stage 1.

The best leg-size solution obtained in the second stage optimization is slightly worse than that found in stage 1. The single-objective solutions are also marked on the figure. Here, the best NSGA-II solution for actuating force is almost identical to the single-objective minimum solution for actuating force, but the individual minimum solution for leg-size obtained by the single-objective GA is worse than that found by the NSGA-II. Importantly, the stage 2 solutions dominate the stage 1 solution by finding solutions smaller in force requirement. This study shows that an identical GA procedure (NSGA-II) is able to treat the leg mechanism optimization problem with and without spring consideration alike.

6.3 Actuating Force and Peak Crank Torque Minimization

Next, we consider the minimization of force and peak crank torque in NSGA-II and the five well-distributed solutions thus obtained are presented in Table 9. These solutions are plotted in Figure 12. Once again, a comparison with results found in stage 1 (without springs) reveals that

Table 8: Minimization of force and leg-size using NSGA-II for the spring-loaded leg mechanism.

	Optimized design solutions						
S.no.	1	2	3	4	5	6	7
x_1 (cm)	4.03	3.79	3.69	3.42	2.88	2.75	2.44
x_2 (cm)	16.08	15.85	15.77	15.03	14.12	14.15	13.94
x_3 (cm)	14.20	14.12	14.11	13.20	13.26	13.26	13.34
x_4 (cm)	11.11	10.25	9.80	9.02	8.01	7.71	7.04
x_5 (cm)	23.57	22.84	22.39	22.62	22.38	22.55	22.78
ϕ (rad)	2.19	2.18	2.18	2.14	2.26	2.26	2.29
s_1 (cm)	-13.75	-10.22	-13.76	-13.54	-9.43	-13.46	-13.34
s_2 (cm)	68.97	68.73	68.05	64.87	64.32	64.21	62.18
k_1 (kN/m)	31.93	19.97	13.82	19.82	22.65	23.05	23.20
k_2 (kN/m)	41.84	45.05	40.48	40.32	40.48	42.34	45.24
l_{01} (cm)	38.55	33.10	35.19	33.98	30.72	34.22	33.68
l_{03} (cm)	22.89	23.98	23.54	22.85	23.15	23.46	22.11
F (kN)	1.39	1.44	1.49	1.57	1.69	1.76	1.89
S	3.11	2.88	2.76	2.62	2.46	2.44	2.39
T (Nm)	4.95	4.30	4.57	3.97	5.04	4.68	4.88

the addition of springs helps achieve solutions requiring smaller torque and forces. Here too, the NSGA-II is able to find a better spread of solutions than that dictated by the single-objective optimization study, mainly due to the difficulty in optimizing a difficult (and non-differentiable) peak crank torque function.

6.4 Force, Leg-size, and Peak Crank Torque Minimization

Finally, we consider all three objectives and five solutions are obtained from the final obtained non-dominated front using NSGA-II. Figure 13 shows these solutions in a three-dimensional objective space. The advantage of using springs is once again very clear from this figure. Once again, the obtained link dimensions here are much smaller compared to those obtained in stage 1 performed without spring elements.

Figure 14 shows the variation of torque with crank angle α for various solutions obtained in Figure 13. It is interesting to note there is a pattern of torque variation in all five trade-off solutions. To become a near-optimal solution, the torque variation is expected to be of certain type over the entire cycle of operation (as depicted in the figure) and to have a trade-off among conflicting objectives, there is some variation of the torque around the mean. This figure shows a remarkable change in pattern in torque variation compared to that in stage 1 (shown in Figure 6).

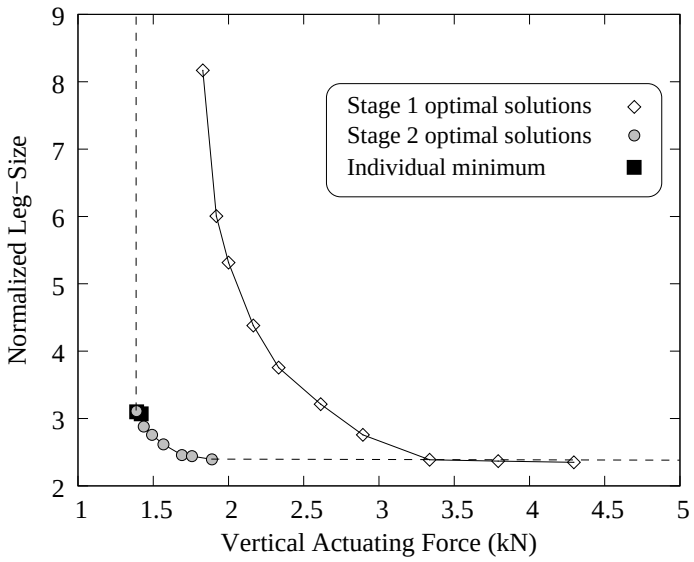

Figure 11: NSGA-II solutions for the minimization of force and leg-size for the spring-loaded leg mechanism.

Table 9: Minimization of force and torque using NSGA-II for the spring-loaded leg mechanism.

	Optimized design solutions				
S.no.	1	2	3	4	5
x_1 (cm)	4.02	3.89	3.81	3.75	3.71
x_2 (cm)	16.06	15.89	15.85	15.96	16.22
x_3 (cm)	14.18	14.18	14.20	14.22	14.23
x_4 (cm)	11.06	10.84	10.56	10.69	11.29
x_5 (cm)	23.55	23.52	23.35	24.11	26.09
ϕ (rad)	2.19	2.19	2.19	2.17	2.14
s_1 (cm)	−13.49	−13.42	−13.41	−12.70	−12.91
s_2 (cm)	68.87	69.07	68.87	68.95	69.35
k_1 (kN/m)	29.77	31.92	29.46	28.73	28.62
k_2 (kN/m)	40.85	42.11	41.75	43.22	44.15
l_{01} (cm)	38.24	38.29	38.07	37.29	37.46
l_{03} (cm)	22.80	23.28	23.29	23.16	22.67
F (kN)	1.39	1.41	1.43	1.45	1.48
S	3.10	3.07	3.00	3.14	3.53
T (Nm)	4.60	4.50	4.27	4.07	3.91

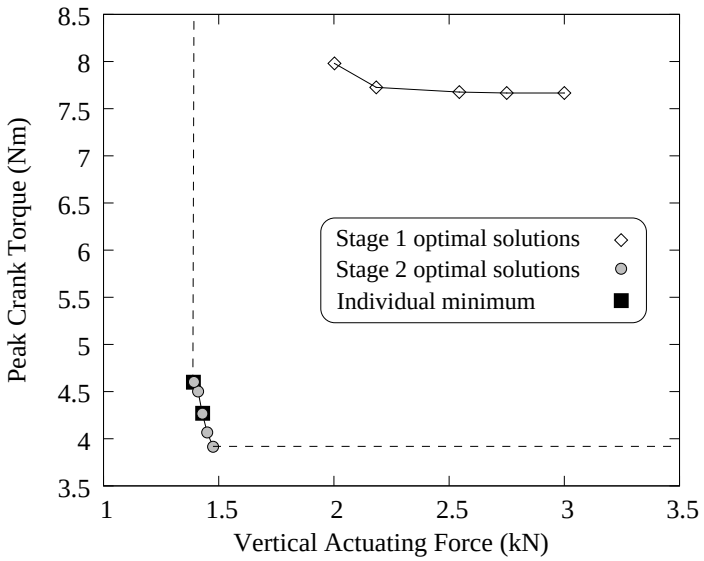

Figure 12: NSGA-II solutions for the minimization of force and torque for spring-loaded leg mechanism.

Table 10: Minimization of all three objectives using NSGA-II for the spring-loaded leg mechanism.

	Optimized Design Solutions				
S.no.	1	2	3	4	5
x_1 (cm)	4.02	3.79	3.73	3.47	3.44
x_2 (cm)	16.06	15.86	15.78	15.03	15.03
x_3 (cm)	14.18	14.12	14.12	13.2	13.2
x_4 (cm)	11.06	10.24	9.96	9.18	9.06
x_5 (cm)	23.53	22.84	22.49	22.68	22.65
ϕ (rad)	2.19	2.18	2.18	2.14	2.14
s_1 (cm)	-13.49	-13.52	-13.67	-13.41	-13.36
s_2 (cm)	68.87	68.73	68.35	66.4	64.93
k_1 (kN/m)	29.77	17.45	18.84	25.93	23.02
k_2 (kN/m)	40.83	45.1	42.28	41.19	39.2
l_{01} (cm)	38.24	35.67	36.26	35.24	34.64
l_{03} (cm)	22.80	23.98	23.70	24.28	22.80
F (kN)	1.39	1.44	1.45	1.54	1.59
S	3.10	2.88	2.79	2.64	2.63
T (Nm)	4.62	4.24	4.10	4.03	3.92

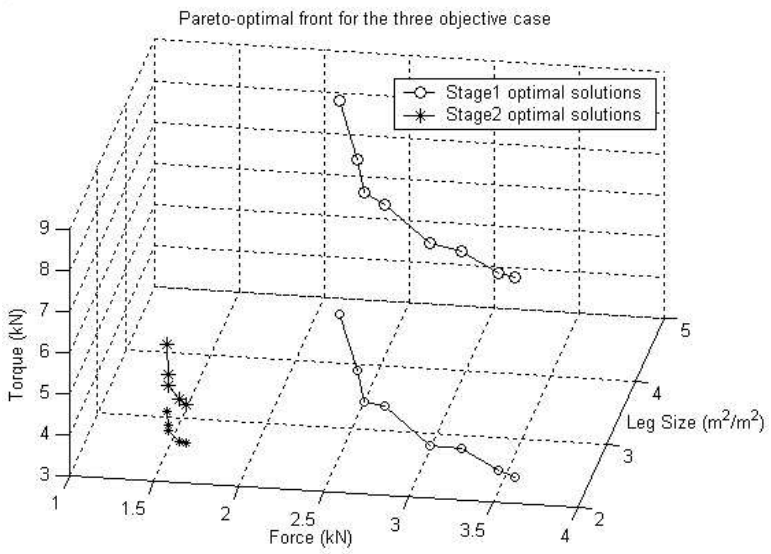

Figure 13: NSGA-II solutions for the minimization of force, leg-size and torque for spring-loaded leg mechanism.

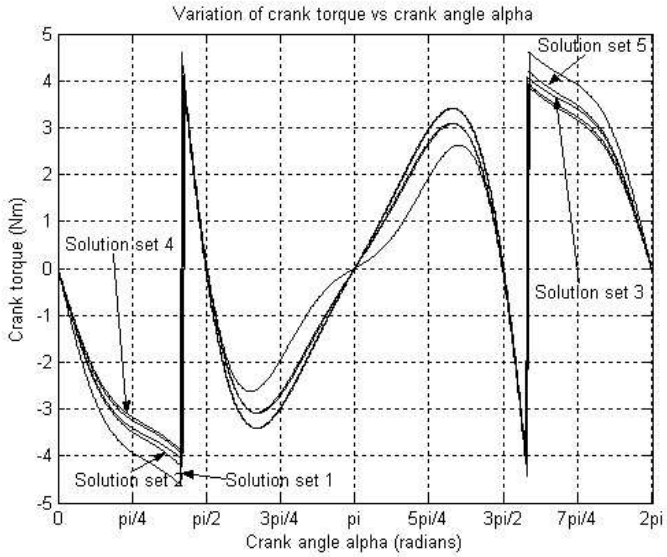

Figure 14: Torque variation with crank angle for all five obtained solutions for the spring-loaded leg mechanism.

7 Conclusions

In this paper, we have made a detailed investigation of a leg mechanism optimization which was performed elsewhere (Shieh et al., 1996). This problem provides a number of challenges to any optimization algorithm: (i) multiple objectives (as many as three), (ii) highly constrained search space (about one in 10^4 random solutions is feasible), (iii) highly non-linear objective and constraint functions and (iv) many linked decision variables. In order to achieve near optimal solutions, the original study divided the problem into two subproblems: (stage 1) without spring elements and (stage 2) with spring elements and performed two independent optimizations. To solve the stage 2 problem, the optimal solution of stage 1 is used and spring elements are only optimized.

In this paper, we have treated the compound leg mechanism problem with spring elements as a whole and have reported optimized solutions for a simultaneous consideration of three different objectives using an evolutionary multi-objective optimization (EMO) procedure. The EMO procedure (NSGA-II) used here is capable of finding multiple Pareto-optimal solutions in a single simulation run, thereby avoiding to use a single-objective optimization technique a number of times, a procedure often followed in classical optimization tasks. Starting from single-objective to two-objective and finally to three-objective optimizations, NSGA-II has demonstrated its flexibility and ability to find near-optimal solutions repeatedly to various versions of the leg mechanism optimization problem. In all cases, better solutions are obtained compared to those reported in the original study.

The extensive use of optimization concepts and a systematic analysis of obtained solutions demonstrated in this paper reveal interesting properties associated with optimal solutions and this study should encourage further use of evolutionary optimization techniques to more complex engineering optimization problems.

References

Deb, K. (2000). An efficient constraint handling method for genetic algorithms. *Computer Methods in Applied Mechanics and Engineering 186*(2–4), 311–338.

Deb, K. (2001). *Multi-objective optimization using evolutionary algorithms.* Chichester, UK: Wiley.

Deb, K. (2003). Unveiling innovative design principles by means of multiple conflicting objectives. *Engineering Optimization 35*(5), 445–470.

Deb, K. and Agrawal, R. B. (1995). Simulated binary crossover for continuous search space. *Complex Systems 9*(2), 115–148.

Deb, K., Agrawal, S., Pratap, A. and Meyarivan, T. (2002). A fast and elitist multi-objective genetic algorithm: NSGA-II. *IEEE Transactions on Evolutionary Computation 6*(2), 182–197.

Deb, K. and Goyal, M. (1998). A robust optimization procedure for mechanical component design based on genetic adaptive search. *Transactions of the ASME: Journal of Mechanical Design 120*(2), 162–164.

Ehrgott, M. (2000). *Multicriteria Optimization.* Berlin: Springer.

Ghosh, A. and Mallik, A. K. (1988). *Theory of Mechanisms and Machines.* New Delhi: Affiliated East-West Press.

Hartenberg, R. and Denavit, J. (1964). *Kinematics Synthesis of Linkages.* New York, NY: McGraw-Hill.

Miettinen, K. (1999). *Nonlinear Multiobjective Optimization.* Boston: Kluwer.

Shieh, W. B., Azaram, S., Tsai, L. W. and Tits, A. L. (1994). Optimization based design of a leg mechanism via combined mechanism and structural analysis. *Advances in Design Automation DE-Vol. 69-1. ASME Pub.*, 199–209.

Shieh, W. B., Azaram, S., Tsai, L. W. and Tits, A. L. (1996). Multi-objective optimization of a leg mechanism with various spring configurations for force reduction. *Journal of Mechanical Design 118*, 179–185.

Williams, R. P., Tsai, L. W. and Azaram, S. (1991). Design of a crank-and-rocker driven pantograph: A leg mechanism for the university of maryland's 1991 walking robot. In *Proceedings of 2nd National Conference on Applied Mechanics and Robotics, Volume 1, No. VIB.2*, Cincinnati, OH.

A Detailed Formulation of the Leg Mechanism

Here we present some additional equations used to formulate the leg mechanism optimization problem. For a complete derivation of the formulae, refer to the earlier study (Shieh et al., 1994). The coordinates of the coupler point E are as follows:

$$X_E = x_1 \sin\alpha \left(\cos\frac{\phi}{2} + V \sin\frac{\phi}{2}\right), \tag{31}$$

$$Y_E = (x_2 - x_1\cos\alpha)\left(\cos\frac{\phi}{2} + V\sin\frac{\phi}{2}\right), \tag{32}$$

where

$$V = \left[\frac{4x_3^2}{x_2^2 - 2x_1x_2\cos(\alpha) + x_1^2} - 1\right]^{1/2}.$$

In the formulation of the expressions involving Y_H we assume that Y_H is held at its mid-range position. The value of Y_H for its mid-range position is given as follows:

$$Y_H = Y_E|_{\alpha=\pi} + \sqrt{2}x_4. \tag{33}$$

The coordinates of foot point J are given as:

$$X_J = -\left(\frac{x_5}{x_4}\right)X_E, \tag{34}$$

$$Y_J = Y_H + \left(\frac{x_5}{x_4}\right)(Y_H - Y_E). \tag{35}$$

The orientation of link 5, θ_5, is given as follows:

$$\theta_5 = \cos^{-1}\left(\frac{X_E}{U}\right) - \cos^{-1}\left(\frac{U}{2x_4}\right), \tag{36}$$

where

$$U^2 = X_E^2 + Y_E^2 + Y_H^2 - 2Y_EY_H.$$